Journal of Chromatography A, 1218 (2011) 5801–5809

Contents lists available at ScienceDirect

Journal of Chromatography A

journal homepage: www.elsevier.com/locate/chroma

Size-exclusion chromatography of perfluorosulfonated ionomers

T.H. Mourey[a,*], L.A. Slater[a], R.C. Galipo[a], R.J. Koestner[b]

[a] Corporate Research and Engineering, Eastman Kodak Company, Rochester, NY 14650-2136, USA
[b] Electrochemical Energy Research Laboratory, General Motors Company, 10 Carriage Street, Honeoye Falls, NY 14472-1039, USA

ARTICLE INFO

Article history:
Received 19 May 2011
Received in revised form 17 June 2011
Accepted 23 June 2011
Available online 30 June 2011

Keywords:
Size-exclusion chromatography
Perfluorosulfonated ionomers
Nafion®
Molar mass
Light scattering
Viscometry
Conformation
Unperturbed dimensions

ABSTRACT

A size-exclusion chromatography (SEC) method in N,N-dimethylformamide containing 0.1 M $LiNO_3$ is shown to be suitable for the determination of molar mass distributions of three classes of perfluorosulfonated ionomers, including Nafion®. Autoclaving sample preparation is optimized to prepare molecular solutions free of aggregates, and a solvent exchange method concentrates the autoclaved samples to enable the use of molar-mass-sensitive detection. Calibration curves obtained from light scattering and viscometry detection suggest minor variation in the specific refractive index increment across the molecular size distributions, which introduces inaccuracies in the calculation of local absolute molar masses and intrinsic viscosities. Conformation plots that combine apparent molar masses from light scattering detection with apparent intrinsic viscosities from viscometry detection partially compensate for the variations in refractive index increment. The conformation plots are consistent with compact polymer conformations, and they provide Mark–Houwink–Sakurada constants that can be used to calculate molar mass distributions without molar-mass-sensitive detection. Unperturbed dimensions and characteristic ratios calculated from viscosity–molar mass relationships indicate unusually free rotation of the perfluoroalkane backbones and may suggest limitations to applying two-parameter excluded volume theories for these ionomers.

© 2011 Elsevier B.V. All rights reserved.

1. Introduction

Polyfluorosulfonated ionomers are copolymers of tetrafluorethylene and sulfonic acid-functionalized (SO_3H) perfluorinated vinyl ethers. DuPont™ developed and commercialized the first perfluorosulfonated ionomer, Nafion® [1], in the mid 1960s. Subsequently, other companies introduced related materials including those shown in Scheme 1. Nafion was originally used in spacecraft fuel cells, and later found applications as membrane materials for the electrolysis production of chlorine and sodium hydroxide, in the production of high purity oxygen and hydrogen, in super-acid catalysis, in the purification of precious metals, in sensors and in a variety of electrochemical applications. Studies on the structure, properties and applications of perfluorosulfonated ionomer membranes were reviewed in 1996 [2] and the state of understanding of Nafion was reviewed in 2004 [3]. In recent years the greatest interest in perfluorosulfonated ionomers has again been for use in fuel cells as a proton conducting polymer in the electrode and separator membrane layers.

The perfluorinated portion of these ionomers imparts exceptional thermal and chemical stability, while the ionic functionality, introduced by the conversion of pendant sulfonyl fluorides ($-SO_2F$) to $-SO_3H$ groups, results in solid-state morphology that provides high proton conductivity. The copolymer composition is expressed in terms of equivalent weight (EW), equal to grams of ionomer per mole of sulfonic acid groups. EW values typically range between EW = 650–1100. Depending on ionomer structure, this corresponds to 13–21 mole% (33–57 wt%) of functionalized comonomer. Ionomer dispersions are prepared at elevated temperatures and pressures at 5–28 wt% ionomer in water/alcohol or water alone. The dispersions can then be cast into membrane materials. Moore and Martin [4] discovered that membrane materials fabricated by simple air drying of Nafion dispersions were soluble in common organic solvents. If instead the dispersion was solvent-exchanged using DMSO or DMF, taken to dryness and then heated at temperatures greater than 100 °C, insoluble membranes with good mechanical properties were obtained.

Aqueous/alcohol perfluorosulfonic acid dispersions of the ionomers form rod-like [5,6] and ribbon-like [7] aggregate structures with perfluorocarbon cores and dissociated sulfonic acid ionic groups exposed to the solvent phase [8]. The influence of ionomer molar mass on the aggregate structure, which in turn influences membrane solid-state morphology, is not fully understood. This

* Corresponding author. Tel.: +1 585 477 5721; fax: +1 5854777781.
E-mail address: thomas.mourey@kodak.com (T.H. Mourey).

0021-9673/$ – see front matter © 2011 Elsevier B.V. All rights reserved.
doi:10.1016/j.chroma.2011.06.078

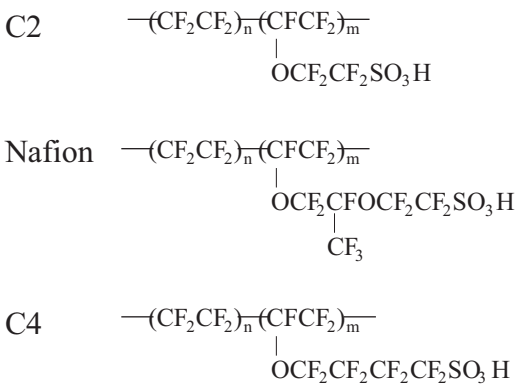

Scheme 1.

may be attributed partially to the lack of molar mass information; these ionomers do not form molecular solutions readily in solvents commonly used for SEC and other forms of polymer dilute solution characterization.

There have been only three reports of SEC of perfluorosulfonated ionomers to our knowledge. Curtin and Lousenberg examined Nafion dispersions by SEC in DMF with light scattering detection [9], and Lousenberg subsequently examined the SEC behavior of Nafion using DMSO with surfactants and an amine as eluent modifiers [10]. A pronounced shoulder was observed in SEC chromatograms at early retention volumes in both DMF and DMSO eluents for dispersion samples that were diluted directly with SEC sample solvent. The shoulder mostly disappeared only after the ionomer dispersions were subjected to autoclaving at temperatures in excess of 230 °C prior to SEC analysis, and the authors mentioned that a small persistent prepeak remained observable in light scattering chromatograms. Autoclaving is an established procedure for breaking aggregate structure and dissolving Nafion membranes that was first introduced by Martin et al. [11]. The specific refractive index increment (dn/dc) of Nafion in both DMF and DMSO is small, resulting in weak differential refractive index (DRI) and light scattering (LS) detector signals. Only one ionomer (Nafion with EW = 1000) was examined and details of the autoclaving procedure were not provided.

Another example of SEC of a perfluorosulfonated ionomer was described as part of a study of membrane degradation [12]. Membranes made from Flemion SH50 (Asahi Glass Company) were dissolved in 80/20 wt% ethanol/water with heating at 120 °C for 16 h. The SEC eluent was methanol containing 50 mM LiCl and the columns were TSK-Gel α-2500 and α-M at an unspecified temperature, and only DRI detection was used. One appealing aspect of this method is that it used a lower dissolution temperature.

This work examines more closely the sample preparation and chromatographic conditions required to obtain true size-exclusion separations of perfluorosulfonated ionomers. The result is a multi-detector SEC method that includes for the first time differential viscometry (DV) detection as well as LS detection. The method is applicable to three different perfluorosulfonated ionomer classes and it provides new information on ionomer conformation in dilute solution.

2. Experimental

2.1. Materials

Nafion perfluorosulfonic acid dispersions were obtained from E.I. du Pont de Nemours and Company (Wilmington, DE). C2 dispersions were obtained from Solvay S.A. (Brussels, Belgium). C4 dispersions were obtained from 3M Corporation (St. Paul, MN).

Table 1
Perfluorosulfonated ionomers.[a]

Ionomer	Class	EW[b]	Solids	H_2O	*n*-PrOH	EtOH	Supplier
D2020 lot#1	Nafion	950	21.6	43.5	56.5	0.0	DuPont
D2020 lot#2	Nafion	1000	21.7	42.5	57.5	0.0	DuPont
D2021	Nafion	1030	20.3	44.2	55.8	0.0	DuPont
D83-20B	C2	830(nom)	19.9	100.0	0.0	0.0	Solvay
3M low EW	C4	825(nom)	18.6	100.0	0.0	0.0	3M
3M high EW	C4	980(nom)	16.3	100.0	0.0	0.0	3M

[a] Solids and solvent fractions are listed as (w/w) %.
[b] Equivalent weight (g/mol) is measured by NaOH titration in aqueous NaCl solution; the nominal EW is reported for three dispersion samples where mineral acid was also present in solution.

Chemical structures are provided in Scheme 1, and the product names, solids content and solvent compositions are listed for these commercial dispersions in Table 1.

2.2. SEC

The SEC system is an Agilent (Santa Clara, CA) 1100 series isocratic pump, autosampler and two-wavelength spectrophotometric detector, an Agilent (formerly Precision Detectors) PD2020 two-angle LS detector, a Malvern (Worchestershire, UK, formerly Viscotek) Model 270 DV detector and a Waters Corporation (Milford, MA) Model 410 DRI detector. The DV and DRI were in a parallel configuration after the spectrophotometric and LS detectors. Three Agilent (formerly Polymer Laboratories) Olexis 7.5 mm × 300 mm columns at 35.0 °C were used with N,N-dimethylformamide (DMF, Omnisolv HPLC grade purchased from EMD Chemicals Gibbstown, NJ) containing 0.1 M $LiNO_3$. The eluent was pre-filtered using 0.22 μm Millipore (Billerica, MA) GS filters. The nominal flow rate was 1.0 mL/min and the actual flow rate was determined from the retention volume in the 270 nm UV chromatogram of 0.2% acetone added to the samples as a flow marker. The columns were calibrated with 15 PMMA narrow standards from Agilent (formerly Polymer Laboratories) with molar masses between 580 and 1,400,000. Injection volumes were 100 μL and the optimum injected sample concentration for samples not subjected to a special solvent exchange procedure discussed below was ~0.5 mg/mL.

The wavelength of the LS detector laser diode is 680 nm. The specific refractive increment (dn/dc) of PMMA at 680 nm was estimated to be 0.062 mL/g by extrapolating the dn/dc values of Mächtle and Fischer [13] for PMMA in DMF at wavelengths between 435.8 nm and 643.8 nm using the Cauchy relation [14]. The peak area response factor of the DRI detector was calculated from PMMA narrow standards and the dn/dc values of perflourosulfonated ionomers were then estimated from their integrated DRI detector responses. The estimated values of dn/dc were independent of sample concentration. The light scattering detector was calibrated with isotropically scattering PMMA standards of known molar mass assuming $dn/dc = 0.062$.

2.3. Sample dissolution

A procedure suitable for the three classes of perfluorosulfonated ionomers shown in Scheme 1 involved diluting ionomer dispersions, which are typically 5–28 wt% solids in water or water/alcohol, to a concentration of ~0.1 wt% in 80/20 *n*-propanol/water (v/v). The original dispersion percent solids and the actual concentrations of the diluted samples were determined gravimetrically. Solid ionomers have densities as high as 2 g/cm^3, so dispersions and solutions were shaken thoroughly during all dilution and transfer steps to ensure homogeneous sampling. Immediately after mixing thoroughly, 8–10 mL of each diluted solution were transferred to a poly(tetrafluorethylene) (PTFE)-lined high-strength acid diges-

tion bomb (model 4746) from Parr Instrument Company (Moline, IL). The Parr bombs were tightened by hand, placed in an oven, heated from 30 to 230 °C at 5 °C per min, and then held for 6 h. Total autoclaving time, including the oven temperature ramp time, was 6 h and 40 min. Due to the metal mass of the bomb vessels, several hours were required to cool the vessels down to room temperature. The bomb vessels were disassembled and the autoclaved solutions were transferred to 20 mL screw cap vials with PTFE-lined caps. The autoclaved solutions were diluted 1:1 (w/w) with SEC sample solvent to give the SEC sample injection concentration of ~0.5 mg/mL.

3. Results and discussion

3.1. SEC optimization

A starting point for the selection of a SEC eluent is to minimize the differences between the solubility parameters of the solvent and the column packing and between the solvent and the solute. This is a bit more complicated for perfluorosulfonated ionomers because they have two solubility parameters. In the case of Nafion with EW = 1200, Yeo [15] determined the cohesive energy density from swelling and calculated a solubility parameter $\delta_1 \sim 9.68$ $(cal/cm^3)^{1/2}$ for the tetrafluoroethylene segments and a second solubility parameter $\delta_2 \sim 16.71$ $(cal/cm^3)^{1/2}$ for the sulfonic acid functionalized comonomer units. The solvents selected by Lousenberg [10] (DMF $\delta = 12.1$ and DMSO $\delta = 12.0$) have solubility parameters between the two Nafion values, but closer to δ_1. Both solvents have larger solubility parameters than polystyrene ($\delta = 9.1$) which is the most common SEC packing for organic eluents. The solubility parameter of methanol ($\delta = 14.5$) selected by Hommura et al. [12] is closer to δ_2. The solubility parameter of the α-M columns used by Hommura is unknown but the hydroxylated methacrylate structure is expected to have a solubility parameter closer to δ_2 than δ_1. Based on this information, some observations on solvent selection attempts can be partially interpreted.

Nafion with EW 950 did not elute from a single α-M column and methanol/50 mM LiCl eluent using the dissolution procedure of Hommura et al. [12]. We did not examine the same ionomer (Flemion) studied by Hommura, and we applied the procedure to a dispersion rather than a cast membrane. It suggests, however, that their dissolution protocol and SEC conditions are not generally applicable to a variety of ionomers. The eluent and column solubility parameters chosen by Hommura are closer to that of the sulfonic acid-functionalized comonomer, which is 33–57 wt% of the copolymer composition. We also attempted to dilute autoclaved and non-autoclaved Nafion (EW = 950) with another common SEC solvent, 1,1,1,3,3,3-hexafluoro-2-propanol, with a solubility parameter $\delta = 17.98$ that is slightly greater than δ_2. Upon careful observation, it was determined that the ionomer sank to the bottom of the vial as a clear insoluble gel phase that could not be examined by SEC. These observations suggest that matching solubility parameters to δ_2 does not appear to lead to robust dissolution and SEC conditions. More closely matching the solubility parameter of the eluent to δ_1 and to the solubility of polystyrene column packing material ($\delta = 9.1$) as is the case with DMF and DMSO, would appear to be a more generally applicable choice.

The addition of lithium salts to DMF SEC eluent is a common practice that arose from early studies on poly(acrylonitrile)s [16]. Aggregate structures create early eluting shoulders and prepeaks in SEC chromatograms [17] that are suppressed by the addition of low concentrations, e.g. 0.01 M, of LiBr or $LiNO_3$. None of the perfluorosulfonated ionomers eluted from the SEC columns using DMF containing 0.01 M $LiNO_3$. Increasing the salt concentration to 0.1 M $LiNO_3$ resulted in complete and reproducible elution of all samples.

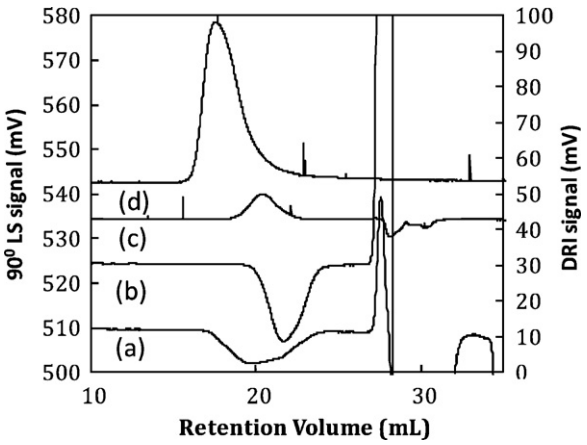

Fig. 1. Chromatograms for Nafion D2020 lot#1 EW = 950 (a) DRI, not autoclaved (b) DRI, autoclaved (c) 90° LS, autoclaved (d) 90° LS, not autoclaved. Autoclave concentration is 0.1 wt% in 80/20 *n*-propanol/water (v/v), 0.5 mg/mL injection concentrations.

We were able to cycle ionomer elution on and off by increasing and decreasing salt concentration from 0.1 M to 0.01 M $LiNO_3$ several times, confirming that higher salt concentration was essential for elution. The nature of the enthalpic interactions between the ionomers and the polystyrene packing material is unknown, but the influence of salt suggests involvement of the sulfonic acid comonomer groups rather than the CF_2 segments.

Samples that are diluted directly with SEC sample solvent (not autoclaved) also elute from Olexis columns with DMF/0.1 M $LiNO_3$ although all three ionomer classes exhibit early eluting shoulders indicative of aggregate structures. The chromatograms of samples diluted directly also exhibited abnormal late elution [18–20] with the light scattering detector measuring large molecules at longer than expected retention volumes. Examples of DRI and LS chromatograms for autoclaved and non-autoclaved Nafion with EW = 950 are shown in Fig. 1. The *u*-shaped *log M* calibration curve symptomatic of late elution calculated from LS detection for the non-autoclaved sample is compared to a more normal looking calibration curve for autoclaved material in Fig. 2. The *u*-shaped calibration curve can also be a symptom of enthalpic interactions of the sample with the column packing. Linear rather than *u*-shaped calibration curves for autoclaved samples along with reproducible chromatograms after multiple sample preparations and injections

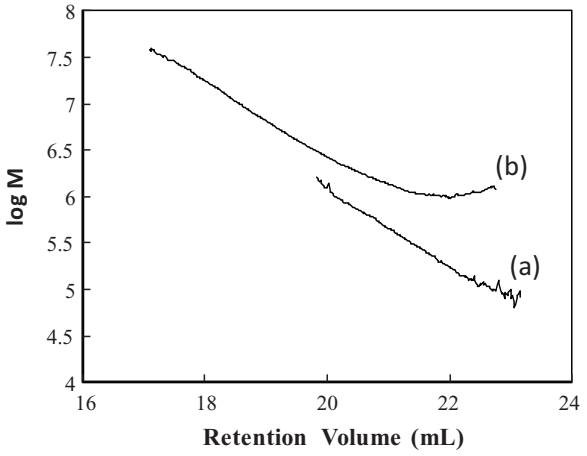

Fig. 2. Calibration curves from LS detection for Nafion D2020 lot#1 (a) autoclaved and (b) not autoclaved. Sample preparation conditions same as Fig. 1.

is additional evidence that 0.1 M $LiNO_3$ largely eliminates sample adsorption to the column packing.

3.2. Ionomer dissolution

The dissolution procedure originally developed by Martin et al. [11] autoclaved 1 wt% ionomer in 50/50 water/*n*-propanol or 50/50 water/ethanol (v/v) at 250 °C for 1 h. We were unable to obtain LS chromatograms without prepeaks at 1 wt% ionomer concentration using 50/50 *n*-propanol/water (v/v) with autoclaving at 260 °C for 1 h, but had some success using 50/50 water/*n*-propanol (v/v) and a lower temperature (230 °C) with longer dissolution time (6 h). These conditions resulted in a coacervate phase for all ionomers, with the bottom phase having higher polymer concentration than the top. The molar mass distributions of the polymers from the two phases were similar. Di-*n*-propyl ether, 1,1-dipropoxypropane and substantial amounts of propene were identified by GC–MS in the autoclaved solutions. The formation of ethers from autoclaving in water–alcohol mixtures was reported by Martin et al. [11] and in a dispersion preparation patent [21], but there is no mention of propene generation. The two-phase autoclaved samples were shaken vigorously before dilution with the SEC sample solvent, resulting in visually clear DMF/0.1 M $LiNO_3$ solutions. Only small prepeaks were observed in LS chromatograms for Nafion with EW 950–1000 but C2 EW 830 and C4 EW 825 exhibited large leading shoulders and prepeaks that indicated aggregate chains remained. Increasing the *n*-propanol/water ratio to 80/20 (v/v) generally led to less evidence of persistent aggregates, particularly in C4 ionomers, but ionomer aggregates were still detected in several ionomer dispersions at 1 wt% autoclaving concentration.

Two phases were obtained for 3M-high EW (C4) for autoclaving concentrations greater than 0.2 wt% in 80/20 propanol/water (v/v), whereas completely clear solutions were obtained at 0.1 wt%. Evidence for aggregates at the higher autoclaving concentrations was not easily detected in DRI chromatograms (Fig. 3) but was readily observed in LS chromatograms (Fig. 4). We also noted that increasing amounts of gaseous product, presumed to include propene, formed at C4 autoclaving concentrations of 0.2 wt% and greater in 80/20 propanol/water (v/v), and created enough pressure to pop the tops off the internal PTFE chambers when the cooled bomb apparatus was disassembled. No appreciable pressurization of the cooled bombs was observed at 0.1 wt% ionomer concentration, which we attribute to less $-SO_3H$ acid-catalyzed *n*-propanol chemistry at lower ionomer concentration. We thus arrived at an optimized autoclaving condition for all three perfluorosulfonated ionomer classes that uses 80/20 *n*-propanol/water (v/v) with 0.1 wt% ionomer concentration. Parenthetically, the optimized autoclaving concentration is near the overlap concentration $c^* \sim 1$ mg/mL reported by Lee et al. in methanol/water [22].

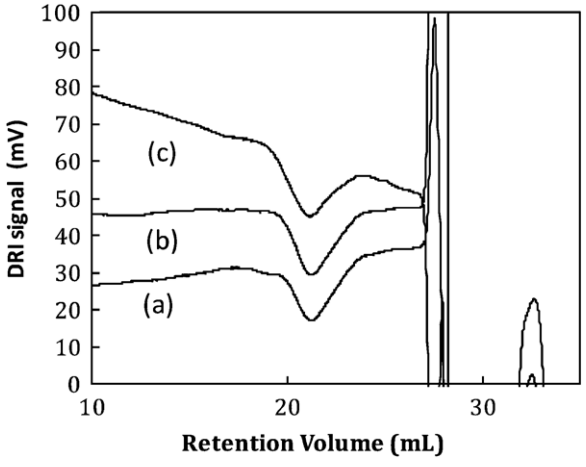

Fig. 3. C4 3 M high EW DRI chromatograms (a) 0.1, (b) 0.2 and (c) 0.4 wt% autoclave concentrations.

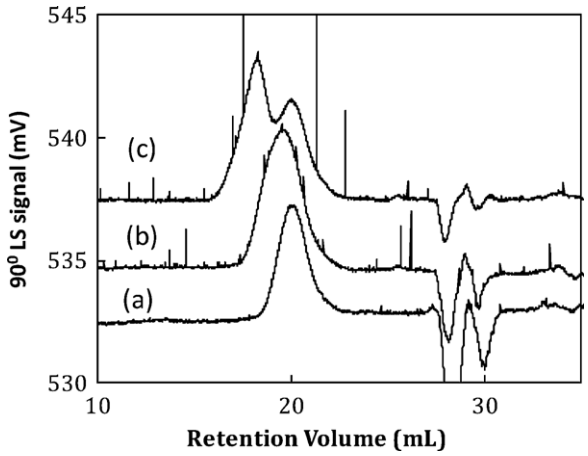

Fig. 4. C4 3 M high EW 90° light scattering chromatograms (a) 0.1, (b) 0.2 and (c) 0.4 wt% autoclave concentrations.

Reproducible chromatograms were obtained for samples autoclaved multiple times using the optimized conditions. Ionomers autoclaved at a higher temperature but for a shorter time (260 °C for 3 h) resulted in chromatograms nearly identical to those obtained using the optimized conditions, but with minor amounts of persistent aggregates observed in light scattering chromatograms. Together, these two observations suggest minimal or no degradation of the ionomers at the optimized autoclaving conditions.

It was claimed recently that molecular solutions are obtained in pure DMF and DMAc after Nafion (EW = 1100) water/alcohol dispersions are evaporated and dried at 60 °C under vacuum [23,24]. Evidence for molecular solutions was inferred from the size and shape of individual particles observed by TEM of frozen solutions. The weight-average molar mass measured by static light scattering was reported as ~255,000 for EW 1100 Nafion, which is in reasonable agreement with our results and those of Lousenberg. Liu et al. [23] examined solutions from 0.1 to 2 mg/mL in pure DMF and DMAc and reported a low second virial coefficient and small root-mean-square radius (22.2 nm) in DMF, consistent with a compact conformation in this solvent. Our SEC chromatogram obtained from dried Nafion ionomer with EW = 1000 that was redissolved in the SEC eluent was intermediate in size between the autoclaved and directly diluted (not autoclaved) Nafion dispersion (Fig. 5). Evidence for extensive aggregation after using this sample preparation method was also observed for a Nafion with EW 950. Although Liu's findings of molecular solution in DMF appear to contradict our results, it must be qualified that the solvents are not the same, i.e. the SEC eluent contains 0.1 M $LiNO_3$ whereas Liu's experiments were in pure DMF.

3.3. Strategies for increasing SEC detector signals

The autoclaved 0.1 wt% solutions were diluted 1:1 (w/w) with SEC sample solvent to avoid a complete mismatch of the injected sample solvent with the eluent. This still results in large solvent peaks and detector signal disruptions in the system peak region. It also introduces relatively low injection concentrations of polymer (0.5 mg/mL). The DRI and LS detector signals are particularly weak at this concentration because of small specific refractive index increments (between −0.02 and −0.04 mL/g), and the viscometry detector signals are weak because of the low intrinsic viscosities of these ionomers. We have had success increasing sample con-

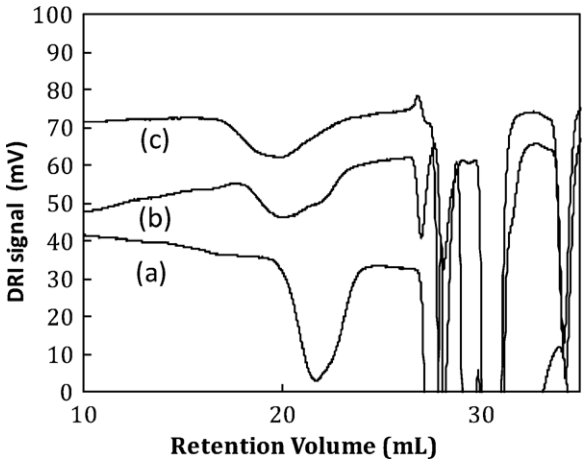

Fig. 5. DRI chromatograms for D2020 lot#2 EW = 1000 (a) autoclaving sample preparation, (b) dispersion taken to dryness and then redissolved with SEC sample solvent and (c) direct dilution of dispersion with SEC sample solvent.

centrations by solvent exchange, akin to the method of Moore and Martin [4]. In this method, 1 g of SEC sample solvent is added to 3 g of 0.1 wt% 80/20 *n*-propanol/water autoclaved solution. The mixed solvent is then partially evaporated with a nitrogen stream to approximately 1.5 g. The lower boiling *n*-propanol and water are preferentially removed while the sample concentration is increased to ~2 mg/mL. The resulting chromatograms show no evidence of aggregate prepeaks or shoulders in light scattering and viscometry detector signals and the shapes of normalized chromatograms are identical to those obtained on samples that are not concentrated by solvent exchange. The procedure is somewhat tedious and requires careful weighing of solutions before and after evaporation to obtain accurate injected sample concentrations. It is also limited to concentrating samples to between 2 and 4 mg/mL depending on ionomer structure, above which re-aggregation occurs. The advantages are a 4× or better improvement of all detector signals as well as a reduction in the water and *n*-propanol peaks observed in the system peak region.

Additional strategies for increasing detector signals are possible. The DV signal can be increased by increasing the flow rate through the detector, although the increase will be limited by the back pressure on the columns and the ratio of the DV and DRI detector split. Alternative solvents such as NMP and DMSO will increase the specific refractive index increment and improve DRI and LS detector signals accordingly, but these solvents also may introduce new complications including the need for elevated temperatures.

3.4. Calculation of molar mass distributions

The calculation of molar mass distributions by light scattering and viscometry detection requires concentrating the autoclaved samples by solvent exchange. Results are provided in Tables 2 and 3. The polymers exhibit little or no light scattering angular dissymmetry. Either the 90 or 15° detector signal can be used to calculate local molar masses, but the root-mean-square radii cannot be calculated for near-isotropic scatterers. The 90° signal is preferred because of better signal-to-noise. Calculating the specific refractive index increment from the calibrated DRI detector response is complicated by differences in light source wavelengths, although it has been demonstrated that calculation of dn/dc at a different wavelength (930 nm pulsed LED for the Waters 410 used in this work) than the light scattering photometer (680 nm for the PD 2020 LS detector) provides acceptable approximations of dn/dc and molar mass calculation [25]. Values of dn/dc are rational compared to Lousenberg's reported value $dn/dc = -0.059$ mL/g for Nafion in DMSO [10]. The latter value was calculated from the calibrated response of a Waters 2410 DRI (we presume it uses an 880 nm source) and is more negative in approximately the correct amount in the slightly higher refractive index solvent, DMSO, than our values in DMF/$LiNO_3$. Liu et al. [23] reported $dn/dc = 0.0196$ mL/g for Nafion in DMF at 514 nm, which is directionally different (positive) relative to our values based on the wavelength dependence for dn/dc, but may reflect the difference between refractive indices of DMF/0.1 M $LiNO_3$ and pure DMF.

Table 2
Light scattering detection.[a]

Ionomer	M_n	M_w	M_z	dn/dc (mL/g)	M_w (no DRI)[b]
D2020 lot#1	184,000	311,000	481,000	−0.033	313,000
D2020 lot#2	190,000	347,000	622,000	−0.030	349,000
D2021	173,000	329,000	603,000	−0.032	331,000
D83-20B	261,000	517,000	906,000	−0.026	516,000
3M low EW	188,000	360,000	605,000	−0.028	365,000
3M high EW	180,000	331,000	597,000	−0.029	333,000
CV (%) $n = 4$	3.5	2.5	6.5	1.8	2.4

[a] Samples solvent exchanged.
[b] Calculated without the DRI detector from the area of the $R(\theta)$ chromatogram and the mass of sample injected.

Table 3
Viscometry detection and Universal Calibration.[a]

Ionomer	M_n	M_w	M_z	$[\eta]$ (dL/g)
D2020 lot#1	198,000	311,000	535,000	0.098
D2020 lot#2	196,000	322,000	467,000	0.095
D2021	217,000	319,000	463,000	0.081
D83-20B	225,000	373,000	605,000	0.202
3M low EW	220,000	336,000	499,000	0.149
3M high EW	168,000	290,000	434,000	0.095
CV (%) $n = 4$	6.7	3.0	5.9	3.5

[a] Samples solvent exchanged.

The coefficients of variation (CV%) reported in Tables 2 and 3 are sample standard deviations divided by the means times 100 for two samples autoclaved 4 separate times and analyzed in duplicate. The agreement between molar mass averages calculated by light scattering and viscometry detection with Universal Calibration presented in Tables 2 and 3 could mislead one into believing that the two methods are in perfect agreement. Calibration curves contain more information. Fig. 6 shows "apparent" calibration curves for a C4 perfluorsulfonated ionomer. The two curves should superim-

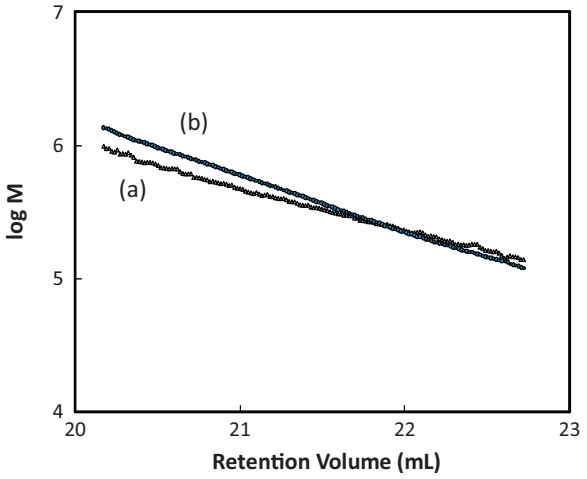

Fig. 6. Apparent log *M* calibration curves for 3M-high EW (C4) using (a) molar mass values calculated from the viscometry detector and the Universal Calibration curve and (b) molar mass values from light scattering detection.

pose if Universal Calibration applies and local concentrations are correctly calculated from the normalized DRI detector response. The crossing of the apparent curves was evident to the same or lesser degrees in all of the ionomers examined. Some conformation plots of $\log M - \log[\eta]$ from viscometry detection where M is calculated from the Universal Calibration curve exhibited curvature and regions with average slopes between 0.8 and 1, unreasonably high for linear, high-molar-mass polymers with comparatively low intrinsic viscosities. Incorrect interdetector volumes and excessive axial dispersion can cause similar calibration curve mismatches and false conformation plots, but these possibilities are ruled out by first obtaining superposition of the $\log M$ calibration curves from viscometry and light scattering detection for a broad distribution PMMA homopolymer on the PMMA narrow standard calibration curve [26].

The mismatched calibration curve problem shown in Fig. 6 can have several origins, but the most common for copolymers is variation in dn/dc across the molecular size distribution caused by comonomer compositional drift. For polymers with very small dn/dc, the variation in absolute units of dn/dc across the molecular size distribution need only be small to have an effect on the calculation of concentration at each retention volume, resulting in an incorrect or apparent molar mass. The apparent local molar mass $M^*_{DV,i}$ at each retention volume i for viscometry detection is

$$\log\ M^*_{DV,i} = \log J_i - \log\left(\frac{\eta_{sp,i}}{c^*_i}\right) \quad (1)$$

where $J_i = M_i[\eta]_i$ is the hydrodynamic volume at retention volume i, obtained from the Universal Calibration curve, and $\eta_{sp,i}/c^*_i = [\eta]^*_i$ is an apparent intrinsic viscosity calculated from the specific viscosity $\eta_{sp,i}$ measured by the viscometry detector and the apparent concentration c^*_i from the normalized DRI detector response. An analogous equation for the apparent molar mass from light scattering for a near-isotropic scatterer with particle scattering function equal to unity, and assuming the concentration is sufficiently low to ignore virial terms is

$$\log M^*_{LS,i} = \log \frac{R(\theta)_i}{k'(dn/dc*)^2_i c^*_i} \quad (2)$$

for Rayleigh scattering $R(\theta)_i$ at retention volume i. The constant k' is the light scattering optical constant, less $(dn/dc^*)^2$. In theory, a corrected concentration and specific refractive index increment at each retention volume can be obtained by equating Eqs. (1) and (2) and minimizing the sum of the squares of the residuals by nonlinear optimization code such as the Solver Excel add-in. The local concentrations are thereby corrected across the chromatogram by accounting for a variation in dn/dc. The estimation of dn/dc and c can only be performed over the data range for which adequate DRI, LS and DV signals are available. In practice, this range can be as small as half the width of the DRI chromatogram. There also is the possibility of more than one solution depending on the optimization procedure and parameters. We applied this approach to the ionomer chromatograms and calculated corrected DRI chromatograms that were not much different than the original chromatograms, partially because the variation in dn/dc across the limited data range appeared to be small.

A simpler alternative to compensate for minor variation in dn/dc across the chromatogram relies on the recognition that the apparent concentration c^*_i is in the denominator of both Eqs. (1) and (2). A conformation plot that uses $\log M^*_{LS,i}$ from light scattering detection with $\log [\eta]^*_i$ from viscometry detection results in the cancellation of c^* in the ordinate and abscissa values, and thereby provides partial rotation of the plot. The slope of the apparent conformation plot using $M^*_{DV,i}$ calculated from viscometry detector and the Universal Calibration curve is $a = 0.846$ (Fig. 7), whereas the slope of the plot

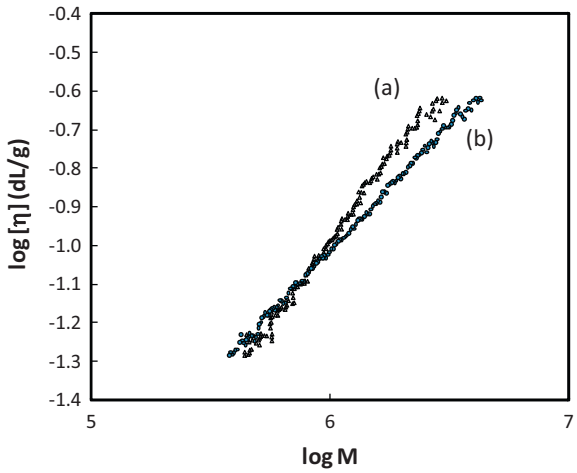

Fig. 7. Conformation plot for 3 M high EW (C4) using (a) molar mass values from the viscometry detector and the Universal Calibration curve and (b) molar mass values from light scattering detection.

using $M^*_{LS,i}$ from light scattering detection on the abscissa and $[\eta]^*_i$ values from viscometry detection on the ordinate is 0.646. The latter is certainly more rational for polymers with comparatively low intrinsic viscosities. The linearity of the plots is also improved for most ionomers when plotting light scattering molar masses on the abscissa, which is additional evidence that the origin of the calibration curve mismatch problem is likely variation in dn/dc across the chromatogram. The calibration curves are rotated closer to correct, but they are recognized as inexact because the plotting procedure does not account for the variation in $(dn/dc^*)_i$ used by Eq. (2).

Mark–Houwink–Sakurada constants from the conformation plots obtained by combining viscosities with molar masses from light scattering detection allow the use of a familiar equation to calculate absolute molar masses from a narrow standard calibration curve and a concentration detector,

$$\log M_2 = 1/(1+a_2)\log(K_1/K_2) + \frac{1+a_1}{1+a_2}\log M_1 \quad (3)$$

where the subscript 1 refers to the narrow standard polymer, e.g. PMMA, and subscript 2 is for the perfluorosulfonated ionomer. Eq. (3) assumes that Universal Calibration is valid. Table 4 contains the molar mass averages calculated from the PMMA calibration curve and the DRI detector using Eq. (3) and the constants are provided in the last two columns of the table. The values for PMMA with molar masses greater than 10,000 are $a_1 = 0.711$ and $K_1 = 9.117 \times 10^{-5}$ (dL/g) in DMF/0.1 M $LiNO_3$ at 35.0 °C. The molecular weight averages are for samples that were not solvent exchanged, and each sample was prepared at least twice and injected in duplicate. The coefficients of variation for molecular weight averages provided at the bottom of the table were obtained from duplicate SEC measurements of D2020 lot #1 samples autoclaved 7 times over a 10-month period. This is a worst case estimate of reproducibility; precision

Table 4
Mark–Houwink calculation method.[a]

Ionomer	M_n	M_w	M_z	a	$K \times 10^5$ (dL/g)
D2020 lot#1	193,000	319,000	515,000	0.684	1.794
D2020 lot#2	204,000	339,000	551,000	0.666	2.080
D2021	211,000	333,000	53,0000	0.673	1.646
D83-20B	232,000	436,000	748,000	0.596	8.638
3M low EW	211,000	357,000	547,000	0.678	2.675
3M high EW	194,000	316,000	495,000	0.646	2.706
CV (%) $n = 7$	4.2	4.2	5.2		

[a] Samples not solvent exchanged (concentration = 0.5 mg/mL).

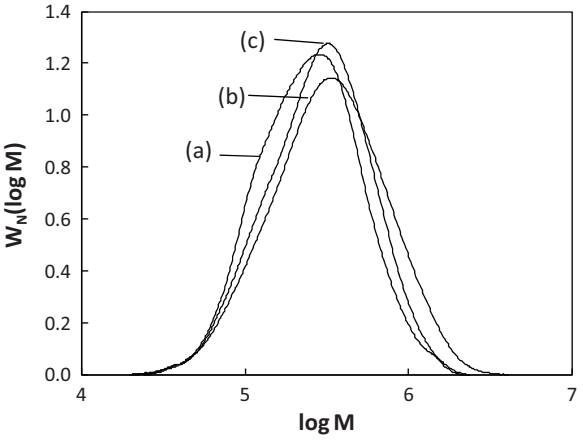

Fig. 8. Differential weight fraction molar mass distributions for three classes of perfluorosulfonated ionomers using Eq. (3). (a) Nafion D2020 lot#1, (b) C2 D83-20B and (c) C4 3M low EW.

is improved for samples run over a short timeframe, i.e. within a fews days of one another. The advantages to the Eq. (3) method are that only a concentration detector is needed and the shapes of molar mass distributions are highly repeatable. Concentration of the samples using the solvent exchange step is also not necessary, but weak DRI signals make baseline setting less certain and may contribute to larger long term variability in molecular weight averages. The error introduced by using the DRI detector response without correction for dn/dc across the chromatogram is small but is nonetheless a disadvantage to this method. Examples of differential weight fraction molar mass distributions calculated by the method utilizing Eq. (3) are shown in Fig. 8 for selected ionomers.

3.5. Polymer conformation and unperturbed dimensions

Conformation plots of the lowest EW members of the three ionomer classes are plotted in Fig. 9. All PFSA ionomers have lower viscosity at equivalent molar mass than linear PMMA. The Mark–Houwink–Sakurada exponents in Table 4 are typical of linear polymers in a fair to good solvent.

The unperturbed dimension parameter $K_\theta = [\eta]_\theta/M^{1/2}$ can be obtained from viscosity-molar mass data in a non-theta solvent using graphical methods based on two-

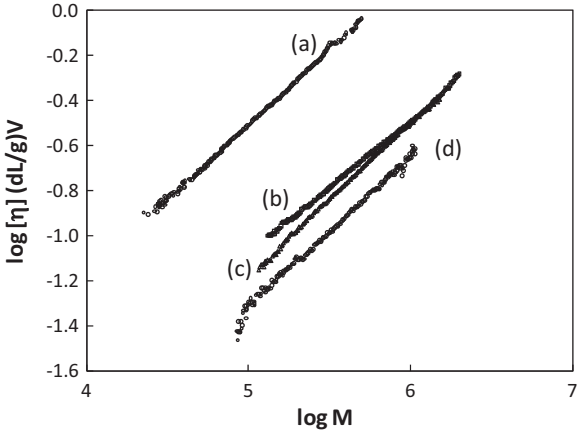

Fig. 9. Conformation plots using light scattering molar masses and viscosities for (a) PMMA broad molecular weight distribution and three classes of ionomers, (b) C2 D83-20B, (c) C4 3M low EW and (d) Nafion D2020 lot#1.

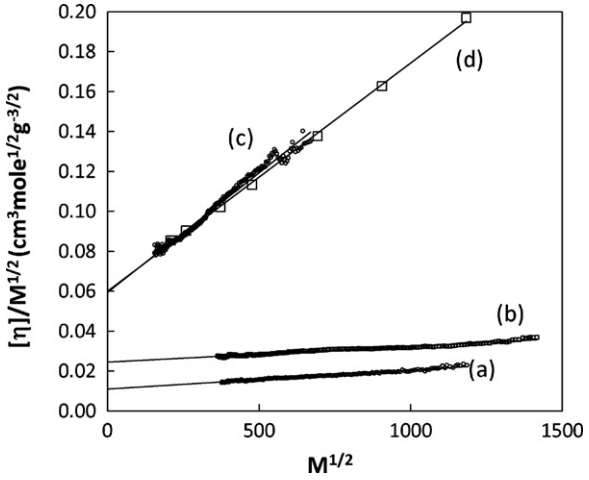

Fig. 10. Viscosity–molar mass data plotted according to Burchard–Stockmayer–Fixman Eq. (4) for (a) Nafion D2020 lot#2, (b) C2 D83-20B and (c) PMMA broad molecular weight distribution (d) PMMA narrow standards.

parameter excluded volume theories. Two methods used frequently are attributed to Burchard–Stockmayer–Fixman [27,28]

$$\frac{[\eta]}{M^{1/2}} = K_\theta + 0.51\Phi_0 B M^{1/2} \tag{4}$$

and Kurata–Stockmayer–Roig [29]

$$\frac{[\eta]^{2/3}}{M^{1/3}} = K_\theta^{2/3} + 0.363\Phi_0 B \left\{ \frac{g(\alpha_\eta)M^{2/3}}{[\eta]^{1/3}} \right\} \tag{5}$$

where Φ_0 is the Flory universal parameter, B is a constant and $g(\alpha_\eta)$ is a function of the linear expansion factor of molecular dimensions due to excluded volume effects. Experimental data indicate the Flory constant varies with solvent and polymer and that $\Phi_0 \sim 2.5 \times 10^{23}\,\mathrm{mol}^{-1}$ is an average estimate [30,31]. K_θ is obtained from the intercept of plots of $M^{1/2}$ vs. $[\eta]M^{-1/2}$ (Eq. (4)) and $M^{2/3}[\eta]^{-1/3}$ vs. $[\eta]^{2/3}M^{-1/3}$ (Eq. (5)). The mean end-to-end distance r_o and characteristic ratio C_n are obtained from the following relationships:

$$K_\theta = \Phi_0 \left(\frac{r_o}{M^{1/2}} \right)^3 \tag{6}$$

$$C_n = \frac{r_o^2}{nl^2 = (r_o/M^{1/2})(m/2l^2)} \tag{7}$$

or the number of bonds n of length $l = 0.154$ nm, and monomer molar mass m. C_n reaches its asymptotic value C_∞ at high values of n, typically a few hundred monomer units. The characteristic ratio is a measure of the effect of short range interactions, which include bond angle restrictions and steric hindrances to internal rotation. The mean-square end-to-end distance r_{of} of the freely rotating vinyl polymer chain consisting of only one kind of bond of length l is

$$r_{of} = 0.308 \left(\frac{M}{m} \right)^{1/2} \tag{8}$$

and the ratio $\sigma = r_o/r_{of}$ represents the effects of steric hindrance on the average chain dimensions. Smaller values of both C_n and σ are indicative of increasingly free bond rotation.

Examples of data plotted in the form of Eq. (4) are provided in Fig. 10. The graphical methods apply only within prescribed upper

Table 5
Unperturbed dimensions.

ID	m^a	K_0 (dL mol$^{1/2}$ g$^{-3/2}$)	$r_o/M^{1/2}$ (nm)	C_n	$r_{of}/M^{1/2}$ (nm)	σ
PMMA	100.0	0.062	0.063	8.4	0.031	2.0
PMMA stds	100.0	0.058	0.061	8.0	0.031	2.0
D2020 lot#1	156.8	0.012	0.036	4.3	0.025	1.5
D2020 lot#2	152.5	0.011	0.036	4.1	0.025	1.4
D2021	149.5	0.010	0.034	3.7	0.025	1.4
D83-20B	127.3	0.024	0.046	5.7	0.027	1.7
3M low EW	163.0	0.017	0.041	5.7	0.024	1.7
3M high EW	149.1	0.012	0.037	4.3	0.025	1.5

[a] Calculated from the weight fractions of comonomers.

limits of the molar mass–viscosity scaling exponent a, and at sufficiently high molar mass. The ionomers in this study appear to satisfy both criteria. The lack of curvature is another measure of the applicability of the theories, and the examples of the most and least linear of all of the data sets are presented. We also applied graphical procedures based on alternative excluded and first-order perturbation theories evaluated by Shashikant et al. [32] and obtained similar estimates for K_θ from all of them. The average of K_θ values obtained from Eqs. (4) and (5) are given in Table 5 along with corresponding values of r_o, r_{of}, C_n and σ. Included are values for PMMA obtained from narrow standards and from a single broad standard using the same graphical methods. The values for PMMA compare favorably to those reported in various solvents, $C_n = 8.65$ and $\sigma = 2.08$ [33], providing some assurance that the graphical procedures can be applied to SEC data. The unperturbed dimension data for the ionomers are suspiciously small. Previous estimates of the characteristic ratio of perfluoroalkane units $C_n = 6.3$ in polyesters indicated that these units are not much more extended than alkane chains [34], but nonetheless the values are larger than most of the values in Table 5, indicating exceptional flexibility in the ionomers. Likewise, characteristic ratios of 7–8 estimated from light scattering of PTFE in perfluorotetracosane also support relatively free rotation of perfluoroalkane backbones [35] but, again, the values are considerably larger than values measured in this work. These previously reported values are for PTFE-like perfluoroalkane units, which are not completely comparable to ionomers because they lack the perfluorosulfonated comonomers. The comonomer content does indeed appear to influence the unperturbed dimensions; the characteristic ratios within the Nafion and C4 classes decrease with increasing equivalent weight, i.e. free rotation increases with decreasing amounts of the sulfonated comonomer. However, the absolute values of the characteristic ratios would rank these ionomers as some of the most flexible polymers known, comparable to highly rotatable polymers containing heteroatoms such as poly(ethylene oxide).

A possible explanation for the low values of C_n and σ is only partial compensation for the variation in dn/dc across the chromatograms by using molar masses from the light scattering detection and intrinsic viscosities from viscometry detection in the calculation of data in Table 5. The C_n and σ values are reported to only two significant figures in Table 5 to respect this concern despite the fact that the error in regression of data plotted in the form given by Eqs. (4) and (5) (Fig. 10) justify three significant figures. However, the intrinsic viscosities reported in Table 3 and the weight-average molar masses reported in Table 2 are whole polymer values that were obtained without the DRI detector; they were calculated from the DV and LS detector signals alone and the mass of sample injected. The exceptionally low viscosities of these ionomers given their relatively high molar mass and small sizes (recall, they are near-isotropic scatterers for the incident wavelength 680 nm) in the SEC solvent is unmistakable. The viscosities are also considerably lower than those of linear PMMA at the same molar mass (Fig. 9). The low viscosities cannot be explained by high molar mass per unit of chain contour length alone; the data instead are more consistent with compact conformations. The majority of our estimates for Mark–Houwink–Sakurada exponents are less than 0.7, which is likewise most consistent with collapsed conformations. Together, the findings may be an indication that the two-parameter excluded volume theories used to calculate unperturbed dimensions in a non-theta solvent may not be suitable for these polymers. These theories account for intramolecular interactions that alter the molecular dimensions from the unperturbed state. The interactions are usually repulsive (excluded volume), resulting in expansion of the polymer coil from its unperturbed Gaussian segment distribution. Perfluorosulfonated ionomers are unusual because of the disparate solubility parameters of their comonomers, and it is possible that there are *attractive* intramolecular forces between comonomers that also affect polymer conformation.

4. Conclusions

The SEC method presented is suitable for three classes of perfluorosulfonated ionomers. The autoclaving procedure provides molecular solutions and the solvent exchange procedure concentrates the samples without re-aggregation, thereby facilitating the use of molar-mass-sensitive detection. There is evidence for minor variation in dn/dc across chromatograms, indicative of copolymer compositional heterogeneity. Slopes of conformation plots and exceptionally low intrinsic viscosities are consistent with a compact polymer conformation in DMF/0.1 M $LiNO_3$. The unperturbed dimensions calculated from SEC viscosity–molar mass data suggest suspiciously free rotation of the perfluoroalkane units, but given the unusual structure and behavior of these materials, this result is an invitation for further study.

Acknowledgements

The authors thank Greg Wolber for assistance with autoclaving procedures.

References

[1] Nafion® is a registered trademark of E.I. du Pont de Nemours.
[2] C. Heitner-Wirguin, J. Membrane Sci. 20 (1996) 1.
[3] K.A. Mauritz, R.B. Moore, Chem. Rev. 104 (2004) 4535.
[4] R.B. Moore, C.R. Martin, Anal. Chem. 58 (1986) 2569.
[5] P. Aldebert, B. Dreyfus, M. Pineri, Macromolecules 19 (1986) 2651.
[6] B. Loppinet, G. Gebel, C.E. Williams, J. Phys. Chem. B 101 (1997) 1884.
[7] L. Rubatat, A.L. Rollet, G. Gebel, O. Diat, Macromolecules 35 (2002) 4050.
[8] S. Jiang, K.-Q. Xia, G. Xu, Macromolecules 34 (2001) 7783.
[9] D.E. Curtin, R.D. Lousenberg, T.J. Henry, P.C. Tangeman, M.E. Tisack, J. Power Sources 131 (2004) 41.
[10] R.D. Lousenberg, J. Polym. Sci. Part B: Polym. Phys. 43 (2005) 421.
[11] C.R. Martin, T.A. Rhoades, J.A. Ferguson, Anal. Chem. 54 (1982) 1639.
[12] S. Hommura, K. Kawahara, T. Shimohira, Y. Teraoka, J. Electrochem. Soc. 155 (2008) A29.
[13] V.W. Mächtle, H. Fischer, Die Angew. Makromol. Chem. 7 (1969) 147.
[14] M.B. Huglin, J. Appl. Polym. Sci. 9 (1965) 4003.
[15] R.S. Yeo, Polymer 21 (1980) 432.
[16] R. Chiang, J.C. Stauffer, J. Polym. Sci. Part A2 5 (1967) 101.
[17] S. Mori, Anal. Chem. 55 (1983) 2414.
[18] S. Podzimek, T. Vlcek, C. Johann, J. Appl. Polym. Sci. 81 (2001) 1588.
[19] E.P.C. Mes, H. de Jonge, T. Klein, R.R. Welz, D.T. Gillespie, J. Chromatogr. A 1154 (2007) 319.
[20] T. Otte, T. Klein, R. Brüll, T. Macko, H. Pasch, J. Chromatogr. A 1218 (2011) 4240.
[21] W.G. Grot, US Patent 4,433,082 February 21, 1984.
[22] S.-J. Lee, T.L. Yu, H.-L. Lin, W.-H. Liu, C.-L. Lai, Polymer 45 (2004) 2853.
[23] W.-H. Liu, T.-Y. Yu, T.L. Yu, H.-L. Lin, e-Polymers 109 (2007) 1.
[24] C.-H. Ma, T.L. Yu, H.-L. Lin, Y.-T. Huang, Y.-L. Chen, U.-S. Jeng, Y.-H. Lai, Y.-S. Sun, Polymer 50 (2009) 1764.
[25] S. Podzimek, in: A.M. Striegel (Ed.), ACS Symposium Series, vol. 893, American Chemical Society, Washington, DC, 2005, p. 94.
[26] T.H. Mourey, S.T. Balke, in: T. Provder (Ed.), ACS Symposium Series, vol. 521. Washington, DC, 1993, pp. 180–198.

[27] W. Burchard, Makromol. Chem. 50 (1961) 20.
[28] W.H. Stockmayer, M. Fixman, J. Polym. Sci. Part C 1 (1963) 137.
[29] M. Kurata, W.H. Stockmayer, A. Roig, J. Chem. Phys. 33 (1960) 151.
[30] H. Fujita, Polymer Solutions, Elsevier, Amsterdam, 1990.
[31] C. Jackson, W.-J. Chen, J.W. Mays, J. Appl. Polym. Sci. 61 (1996) 865.
[32] S. Shashikant, C.K. Patel, P.N. Chaturvedi, Polymer 33 (1992) 4569.
[33] J. Brandrup, E.H. Immergut, E.A. Grulke (Eds.), Polymer Handbook, 4th ed., John Wiley and Sons, New York, 1999.
[34] K. Matsuo, W.H. Stockmayer, G.F. Needham, J. Polym. Sci. Polym. Symp. 71 (1984) 95.
[35] B. Chu, C. Wu, W. Buck, Macromolecules 22 (1989) 831.